

Models of spherical shells as sources of Majumdar-Papapetrou type spacetimes

Gonzalo García-Reyes*

Departamento de Física, Universidad Tecnológica de Pereira, A. A. 97, Pereira, Colombia

By starting with a seed Newtonian potential-density pair we construct relativistic thick spherical shell models for a Majumdar-Papapetrou type conformastatic spacetime. As a simple example, we consider a family of Plummer-Hernquist type relativistic spherical shells. As a second application, these structures are then used to model a system composite by a dust disk and a halo of matter. We study the equatorial circular motion of test particles around such configurations. Also the stability of the orbits is analyzed for radial perturbation using an extension of the Rayleigh criterion. The models considered satisfying all the energy conditions.

* e-mail: ggarcia@utp.edu.co

I. INTRODUCTION

Spherically symmetric distribution of matter are important in astrophysics as models of globular clusters, elliptical galaxies, galactic bulges and dark matter haloes. Spherical shells models are also useful tools in astrophysics and general relativity as sources of vacuum gravitational fields, cosmological models, gravitational collapse, and supernovae [1, 2]. The pioneering work on relativistic shells is due to Israel [3], who also specialized his general framework to spherical symmetry [4]. Relativistic spherical shells with varying thickness were studied in [5–7] for a Schwarzschild type conformastatic spacetime.

Thin shells representing the field of a disk are of astrophysical importance in modeling galaxies, accretion disks, and the superposition of a black hole and a galaxy. Static thin disks without radial pressure were first studied by Bonnor and Sackfield [8], and Morgan and Morgan [9], and with radial pressure also by Morgan and Morgan [10]. Several classes of exact solutions of the Einstein field equations corresponding to static thin disks with or without radial pressure have been obtained by different authors [11–17]. Rotating thin disks that can be considered as a source of a Kerr metric were presented by Bičák and Ledvinka [18], while rotating disks with heat flow were studied by González and Letelier [19]. The exact superposition of a disk and a static black hole was first considered by Lemos and Letelier in Refs. [20, 21]. Disk-like matter distribution surrounded by a material halo for conformastatic spacetimes have been studied in [22] and for Einstein-Maxwell fields in [23] and [24]. Axisymmetric conformastatic disk-haloes were also considered in [25] from solutions of Laplace's equation.

In this work, we construct models of spherically symmetric thick shells for a Majumdar-Papapetrou type conformastatic spacetime from a Newtonian potential-density pair (Poisson's equation). The method used allows to model different spherically symmetric astrophysical systems such as galactic nuclei and certain star clusters where relativistic effects are expected to have a significant impact. As a simple example, we consider a family of Plummer-Hernquist type relativistic spherical shells. Besides shells, the potential-density pair considered permits to model configurations of matter with a central cusp and with a finite central density. As a second application, these structures are then used to model dust disk surrounded of haloes of matter. The distributions of matter studied are essentially of infinite extension. However, since the energy density decreases rapidly one can define a cut off radius and, in principle, to consider these objects as finite.

The paper is organized as follows. In Sect. II we present the method to construct different spherical configurations of matter from a Newtonian potential-density pair in the particular case of a Majumdar-Papapetrou type conformastatic spacetime. In Sect. III the formalism is employed to build a family of Plummer type relativistic spherical shell, and then in Sect. IV we model from them a system composite by a dust disk and a halo of matter. In each case we study the equatorial circular motion of test particles around the structures. Also the stability of the orbits is analyzed for radial perturbation using an extension of the Rayleigh criterion [26, 27]. Finally, in Sect. V we summarize and discuss the results obtained.

II. MAJUMDAR-PAPAPETROU TYPE FIELDS AND SPHERICAL STRUCTURES

We consider a conformastatic spacetime [28, 29] in spherical coordinates (t, r, θ, φ) and in the particular form

$$ds^2 = -f dt^2 + f^{-1}(dr^2 + r^2 d\Omega), \quad (1)$$

where $f(r)$ and $d\Omega = d\theta^2 + \sin^2 \theta d\varphi^2$. These fields can be called Majumdar-Papapetrou type fields due to its known use in context of electrostatic fields [30, 31]. Making $f = (1 - \Phi/2)^{-4}$, with $\Phi(r)$, the same metric takes the form

$$ds^2 = - \left(1 - \frac{\Phi}{2}\right)^{-4} dt^2 + \left(1 - \frac{\Phi}{2}\right)^4 (dr^2 + r^2 d\Omega). \quad (2)$$

The Einstein field equations $G_{ab} = 8\pi G T_{ab}$ yield the following non-zero components of the energy-momentum tensor

$$T^t_t = - \frac{\nabla^2 \Phi}{4\pi G \left(1 - \frac{\Phi}{2}\right)^5}, \quad (3a)$$

$$T^\theta_\theta = T^\varphi_\varphi = \frac{\nabla \Phi \cdot \nabla \Phi}{8\pi G \left(1 - \frac{\Phi}{2}\right)^6}, \quad (3b)$$

$$T^r_r = - \frac{\nabla \Phi \cdot \nabla \Phi}{8\pi G \left(1 - \frac{\Phi}{2}\right)^6}. \quad (3c)$$

In terms of the orthonormal tetrad $e_{(a)}^b = \{V^b, X^b, Y^b, Z^b\}$, where

$$V^a = f^{-1/2} \delta_t^a, \quad X^a = f^{1/2} \delta_r^a, \quad (4a)$$

$$Y^a = \frac{f^{1/2}}{r} \delta_\theta^a, \quad Z^a = \frac{f^{1/2}}{r \sin \theta} \delta_\varphi^a, \quad (4b)$$

the energy-momentum tensor can be written as

$$T^{ab} = \rho V^a V^b + p_r X^a X^b + p_\theta (Y^a Y^b + Z^a Z^b), \quad (5)$$

so that the energy density is given by $\rho = -T^t_t$, and the stresses (pressure or tensions) by $p_i = T^i_i$. In order to have a physically meaningful matter distribution the components of the energy-momentum tensor must satisfy the energy conditions. The weak energy condition requires that $\rho \geq 0$, whereas the dominant energy condition states that $|\rho| \geq |p_i|$. The strong energy condition imposes the condition $\rho_{eff} = \rho + p_r + p_\theta + p_\varphi \geq 0$, where ρ_{eff} is the “effective Newtonian density”.

The metric function Φ can be chosen by requiring that in the Newtonian limite $\Phi \ll 1$ the expression for the relativistic energy density must reduce to Poisson’s equation

$$\nabla^2 \Phi_N = 4\pi G \rho_N. \quad (6)$$

This condition is satisfied by taking $\Phi = \Phi_N$.

Thus, the physical quantities associated with the matter distribution are given by

$$\rho = \frac{\rho_N}{\left(1 - \frac{\Phi_N}{2}\right)^5}, \quad (7a)$$

$$p_\theta = p_\varphi = -p_r = \frac{\nabla \Phi_N \cdot \nabla \Phi_N}{8\pi G \left(1 - \frac{\Phi_N}{2}\right)^6}, \quad (7b)$$

and the average pressure by

$$p = \frac{1}{3}(p_r + p_\theta + p_\varphi) = \frac{\nabla \Phi_N \cdot \nabla \Phi_N}{24\pi G \left(1 - \frac{\Phi_N}{2}\right)^6}. \quad (8)$$

In conclusion, given a seed Newtonian potential-density pair (Φ_N, ρ_N) we can constructed for conformastatic fields different models of spherical compact objects such as spheres, spherical shells, disks and haloes.

A. Motion of particles and stability

We will now analyze the motion of test particles around the structures on the plane $\theta = \pi/2$. For equatorial circular orbits the 4-velocity u^a of the particles with respect to the coordinates frame has components $u^a = u^t(1, 0, 0, \omega)$ where $\omega = u^\varphi/u^t = \frac{d\varphi}{dt}$ is the angular speed of the test particles. For the spacetime (2), the equation for the geodesic motion of the particle is given by

$$g_{ab,r} u^a u^b = 0, \quad (9)$$

from which we get

$$\omega^2 = -\frac{g_{tt,r}}{g_{\varphi\varphi,r}}. \quad (10)$$

On the other hand, u^t obtains normalizing u^a , that is requiring $g_{ab} u^a u^b = -1$, so that

$$(u^t)^2 = -\frac{1}{g_{\varphi\varphi}\omega^2 + g_{tt}}. \quad (11)$$

With respect to the orthonormal tetrad (4a)-(4b) the 3-velocity has components

$$v^{(i)} = \frac{e^{(i)}_a u^a}{e^{(0)}_b u^b}. \quad (12)$$

For equatorial circular orbits the only nonvanishing velocity component is given by

$$(v^{(\varphi)})^2 = v_c^2 = -\frac{g_{\varphi\varphi}}{g_{tt}}\omega^2, \quad (13)$$

which represents the circular speed (rotation profile) of the particle as seen by an observer at infinity. Thus we obtain

$$v_c^2 = \frac{rf_{,r}}{2f - rf_{,r}}. \quad (14)$$

Another quantity related with the geodesic motion of the particles is the specific angular momentum of a particle rotating at a radius r , defined as $h = g_{\varphi\varphi}u^\varphi$. For the plane $\theta = \pi/2$, we have

$$h^2 = \frac{r^2 f^{-1} v_c^2}{1 - v_c^2}. \quad (15)$$

This quantity can be used to analyze the stability of the particles against radial perturbations. The condition of stability,

$$\frac{d(h^2)}{dr} > 0, \quad (16)$$

is an extension of the Rayleigh criteria of stability of a fluid in rest in a gravitational field [27].

For the above spherical distribution these quantities give

$$v_c^2 = \frac{v_{Nc}^2}{1 - \frac{\Phi_N}{2} - v_{Nc}^2}, \quad (17a)$$

$$h^2 = \frac{r^2(1 - \frac{\Phi_N}{2})^4 v_{Nc}^2}{1 - \frac{\Phi_N}{2} - 2v_{Nc}^2}, \quad (17b)$$

where $v_{Nc}^2 = r\Phi_{N,r}$ is the Newtonian circular speed.

III. PLUMMER-HERNQUIST TYPE SPHERICAL SHELL MODELS

A simple Newtonian potential-density pair is [5]

$$\Phi_N = -\frac{GM}{(r^n + a^n)^{1/n}}, \quad (18a)$$

$$\rho_N = \frac{M(n+1)a^n r^{n-2}}{4\pi(r^n + a^n)^{2+1/n}}, \quad (18b)$$

where a is a non-zero constant with the dimension of length and $n \geq 1$. For $n = 1$ the potential-density pair (18a) and (18b) reduces to Hernquist model which has a density profiles with a central cusp and it has been used to model elliptical galaxies and bulges [32]. For $n = 2$ we have the Plummer's spherical model [33, 35] for globular clusters which has a mass distribution concentrated at center. This potential-density pair has also been used to model the central region of our Galaxy composed by the bulge/stellar-halo and the inner core [34]. For $n \geq 3$ we have a shell-like matter distribution. The Newtonian circular speed is given by

$$v_{Nc}^2 = \frac{GM r^n}{(r^n + a^n)^{1+1/n}}. \quad (19)$$

In this case the metric function f is given by

$$f = \left[1 + \frac{GM}{2} (r^n + a^n)^{-1/n} \right]^{-4}, \quad (20)$$

and the relativistic expressions for the physical quantities main associated with the matter distributions are

$$\rho = \frac{8(1+n)\tilde{a}^n\tilde{r}^{n-2}}{\pi G^3 M^2 \xi^{2-4/n} (2\xi^{1/n} + 1)^5}, \quad (21a)$$

$$p = \frac{8\tilde{r}^{2n-2}\xi^{4/n-2}}{3\pi G^3 M^2 (2\xi^{1/n} + 1)^6}, \quad (21b)$$

$$v_c^2 = \frac{2\tilde{r}^n}{2\xi^{1/n+1} + \xi - 2\tilde{r}^n}, \quad (21c)$$

$$h^2 = \frac{G^2 M^2 \tilde{r}^{2+n} (2\xi^{1/n} + 1)^2}{2\xi^{2/n} (2\xi^{1/n+1} + \xi - 4\tilde{r}^n)}, \quad (21d)$$

where $\tilde{r} = r/(MG)$, $\tilde{a} = a/(MG)$, and $\xi = \tilde{r}^n + \tilde{a}^n$.

In Figures 1 - 2 we plot, as functions of \tilde{r} , the energy density $\tilde{\rho} = G^3 M^2 \rho$ and the average pressure $\tilde{p} = G^3 M^2 p$ for the Hernquist-like model $n = 1$, the Plummer-like model $n = 2$, and the relativistic spherical shells $n = 3$ and $n = 6$, with parameter $\tilde{a} = 1, 1.5$ and 2 . When $n = 1$ we have a cusp-like density profile, when $n = 2$ we have a finite central density, and when $n > 2$ the density profile vanishes at the origin which suggests a shell-like matter distribution. In all cases, the energy density decreases rapidly with \tilde{r} which permits to define a cut off radius r_c and, in principle, to consider these structures as compact objects. The shells become more concentrated when the parameter a is increased. We also find that the energy is everywhere positive in accordance with the weak energy condition and we have positive stresses (pressure).

In Figures 3 - 4 we show the curves of tangential speed (rotation curves) v_c and the specific angular momentum $\tilde{h} = h/(GM)$ for the same value of the parameters, as functions of \tilde{r} . We observe that the rotation curves are not flat which means that these configurations of matter can only model, as in the case $n = 1$ and $n = 2$, the visible matter presents in the central regions of the galaxies such as the galactic bulge and the inner core where the relativistic effect can be important and the observed rotation curves have a behavior similar to those shown in figures [34]. We also see that the speed of the particles always is less than light speed in agreement the dominant energy condition. When the parameter a is increased the motion of the particles becomes less relativistic and can stabilize the orbits against radial perturbation. Thus, except the shell $n = 6$ and parameter $a = 1$, these structures have a physically reasonable behavior.

IV. DUST DISKS SURROUNDED BY HALOES

Exact solutions of the Einstein field equations which represent the field of a disk can be obtained by writing the metric (2) in cylindrical coordinates (t, R, z, φ)

$$ds^2 = -f(R, z)dt^2 + f(R, z)^{-1}(dR^2 + dz^2 + R^2 d\varphi^2), \quad (22)$$

and using the well known “displace, cut and reflect” method that was first used by Kuzmin [36] and Toomre [37] to constructed Newtonian models of disks, and later extended to general relativity [15, 16, 18, 19]. Given a solution of the Einstein’s equations, this procedure is mathematically equivalent to apply the transformation $z \rightarrow |z| + z_0$, with z_0 constant. The method is the gravitational version of the method of images of electrostatic.

The content of matter on the disks can be analyzed using the formalism of distributions in curved spacetimes [3, 4, 38–40]. For the metric (22) obtains a dust (zero pressure) disk with surface energy density [41]

$$\epsilon = \frac{1}{4\pi G} f^{-1/2} f_{,z}. \quad (23)$$

In addition, the tangential speed v_c and the specific angular momentum h for geodesic motion of test particles on the disks plane are given by

$$v_c^2 = \frac{R f_{,R}}{2f - R f_{,R}}, \quad (24a)$$

$$h^2 = \frac{R^2 f^{-1} v_c^2}{1 - v_c^2}. \quad (24b)$$

All the quantities are evaluated at $z = 0^+$.

Now when this procedure is applied to the above structures with $0 \leq z_0 \leq r_c$, one obtains at points with $z > 0$ a matter spherical cap corresponding to a sphere with center located at point $(R, z) = (0, -z_0)$, and when $z < 0$ a matter cap of a sphere with center at $(R, z) = (0, z_0)$. The discontinuity in the normal derivative of the metric tensor through the plane $z = 0$ introduces a planar matter distribution which is interpreted as the field of a thin disk. The result in this case is a system composite by dust disks surrounded by a halo of matter (figure 5).

For the potential-density pair (18a) and (18b) we have

$$f = \left[1 + \left([\tilde{R}^2 + (|\tilde{z}| + \tilde{z}_0)^2]^{n/2} + \tilde{a}^n \right)^{-1/n} \right]^{-4}, \quad (25)$$

where $\tilde{R} = R/(GM)$, $\tilde{z} = z/(GM)$, $\tilde{z}_0 = z_0/(GM)$, $\tilde{a} = a/(GM)$, and the surface density energy is

$$\epsilon = \frac{4\tilde{z}_0\tilde{r}^{n-2}(\tilde{r}^n + \tilde{a}^n)^{2/n-1}}{\pi G[2(\tilde{r}^n + \tilde{a}^n)^{1/n} + 1]^3}, \quad (26)$$

where $\tilde{r} = \sqrt{\tilde{R}^2 + \tilde{a}^2}$.

In Fig. 6 we show the surface energy density $\tilde{\epsilon} = G\epsilon$, the tangential speed v_c and the specific angular momentum $\tilde{h} = h/(GM)$ for disks with $n = 2, 3, 6$ and parameters $\tilde{a} = \tilde{z}_0 = 1$, as functions of \tilde{R} . We see that the energy is everywhere positive, its maximum occurs in the center of the disk, and it vanishes sufficiently fast as \tilde{R} increases. When the parameter n is increased, the energy density increases. We observe that circular speed of particles is always a quantity less than the speed of light and that the increasing of n makes more relativistic the orbits. We also see that the rotation curves are not flat which means that these structures can only model the luminous matter of galaxies. In addition, in all cases the motion of particles is stable against radial perturbation. The same behavior is observed for other values of parameter.

V. DISCUSSION

Spherical shell models for a Majumdar-Papapetrou type conformastatic spacetime was constructed, using as seed a Newtonian potential-density pair. The formalism presented allows to construct different relativistic spherical configurations of matter such as spheres and shell-like configurations. The method was illustrated in the case of a family of Plummer-Hernquist type relativistic thick spherical shells. Besides shells, this potential-density pair also permits to construct configurations of matter with a central cusp and with a finite central density. These structures were then used to study models of dust disks surrounded by a halo of matter. The models considered satisfied all the energy conditions.

REFERENCES

-
- [1] J. Kijowski, G. Magli and D. Malafarina, *Gen. Relativ. Gravit.* **38**, 1697 (2006).
 - [2] J. Kijowski, G. Magli and D. Malafarina, *Int. J. Mod. Phys. D* **18**, No. 12, 1801 (2009).
 - [3] E. Israel, *Nuovo Cimento* **44B**, 1 (1966).
 - [4] E. Israel, *Nuovo Cimento* **48B**, 463 (1967).
 - [5] D. Vogt and P. S. Letelier, *Mon. Not. Roy. Astron. Soc.* **402**, 1313 (2010).
 - [6] D. Vogt and P. S. Letelier, *Mon. Not. Roy. Astron. Soc.* **406**, 2689 (2010).
 - [7] P. H. Nguyen, M. Lingam, *Mon. Not. Roy. Astron. Soc.* **436**, 3, 2014 (2013).
 - [8] W. A. Bonnor and A. Sackfield, *Commun. Math. Phys.* **8**, 338 (1968).
 - [9] T. Morgan and L. Morgan, *Phys. Rev.* **183**, 1097 (1969).
 - [10] L. Morgan and T. Morgan, *Phys. Rev. D* **2**, 2756 (1970).
 - [11] D. Lynden-Bell and S. Pineault, *Mon. Not. R. Astron. Soc.* **185**, 679 (1978).
 - [12] A. Chamorro, R. Gregory, and J. M. Stewart, *Proc. R. Soc. London* **A413**, 251 (1987).
 - [13] P. S. Letelier and S. R. Oliveira, *J. Math. Phys.* **28**, 165 (1987).
 - [14] J. P. S. Lemos, *Class. Quantum Grav.* **6**, 1219 (1989).
 - [15] J. Bičák, D. Lynden-Bell, and J. Katz, *Phys. Rev. D* **47**, 4334 (1993).
 - [16] J. Bičák, D. Lynden-Bell, and C. Pichon, *Mon. Not. R. Astron. Soc.* **265**, 126 (1993).

- [17] G. A. González and O. A. Espitia, Phys. Rev. D **68**, 104028 (2003).
- [18] J. Bičák and T. Ledvinka, Phys. Rev. Lett. **71**, 1669 (1993).
- [19] G. A. González and P. S. Letelier, Phys. Rev. D **62**, 064025 (2000).
- [20] J. P. S. Lemos and P. S. Letelier, Class. Quantum Grav. **10**, L75 (1993).
- [21] J. P. S. Lemos and P. S. Letelier, Phys. Rev. D **49**, 5135 (1994).
- [22] D. Vogt and P. S. Letelier, Phys. Rev. D **68**, 084010 (2003).
- [23] A. C. Gutiérrez-Piñeres, G. A. González, and H. Quevedo, Phys. Rev. D **87**, 044010 (2013).
- [24] A. C. Gutiérrez-Piñeres, Gen. Relativ. Gravit. **47**, No. 5, 54 (2015).
- [25] G. A. González and O. M. Pimentel, Phys. Rev. D **93**, 044034 (2016).
- [26] Lord Rayleigh, 1917, Proc. R. Soc. London A, **93**, 148
- [27] L. D. Landau and E. M. Lifshitz, *Fluid Mechanics*(Addison-Wesley, Reading, MA, 1989).
- [28] J. L. Synge, Relativity: The General Theory (North- Holland, Amsterdam, 1966).
- [29] H. Stephani, D. Kramer, M. McCallum, C. Hoenselaers, and E. Herlt, Exact Solutions of Einsteinss Field Equations (Cambridge University Press, Cambridge, England, 2003).
- [30] S. D. Majumdar, Phys. Rev. **72**, 390 (1947).
- [31] A. Papapetrou , Proc. Roy. Soc. (London) **A51**, 191 (1947).
- [32] L. Hernquist, Ap. J., **356**, 359 (1990).
- [33] H. C. Plummer, MNRAS **71**, 460 (1911).
- [34] C. Flynn, J. Sommer-Larsen and P. R. Christensen, MNRAS, **281**, 1027 (1996).
- [35] J. Binney J and S. Tremaine S, 2008, Galactic Dynamics, 2nd edn. Princeton Univ. Press, Princeton, NJ.
- [36] G. G. Kuzmin 1956, Astron. Zh., **33**, 27 (1956).
- [37] A. Toomre, Ap. J., **138**, 385 (1962).
- [38] A. Papapetrou and A. Hamouni, Ann. Inst. Henri Poincaré **9**, 179 (1968)
- [39] A. Lichnerowicz, C.R. Acad. Sci. **273**, 528 (1971)
- [40] A. H. Taub, J. Math. Phys. **21**, 1423 (1980)
- [41] G. García-Reyes and O. A. Espitia, Gen. Relativ. Gravit. **46**, 1674 (2014).

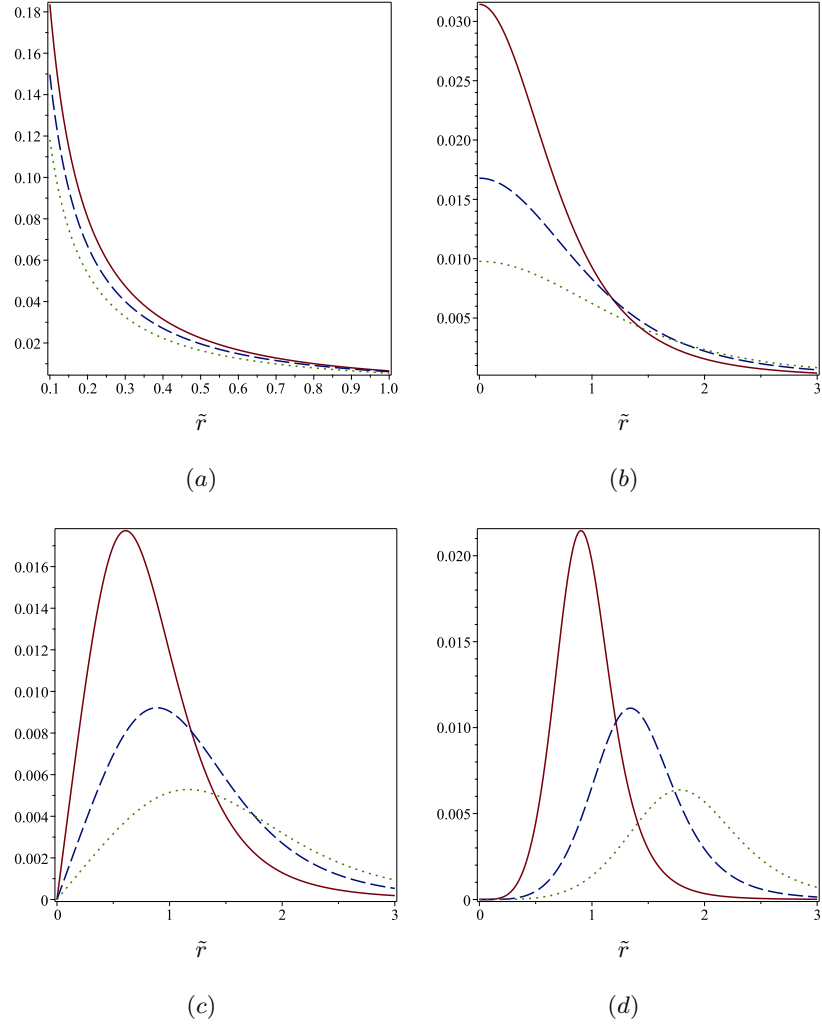


FIG. 1. The relativistic energy density $\tilde{\rho}$, as function of \tilde{r} , for (a) the Hernquist-like model $n = 1$, (b) the Plummer-like model $n = 2$, and the shells (c) $n = 3$ and (d) $n = 6$, with parameter $\tilde{a} = 1$ (solid curves), 1.5 (dashed curves) and 2 (dotted curves).

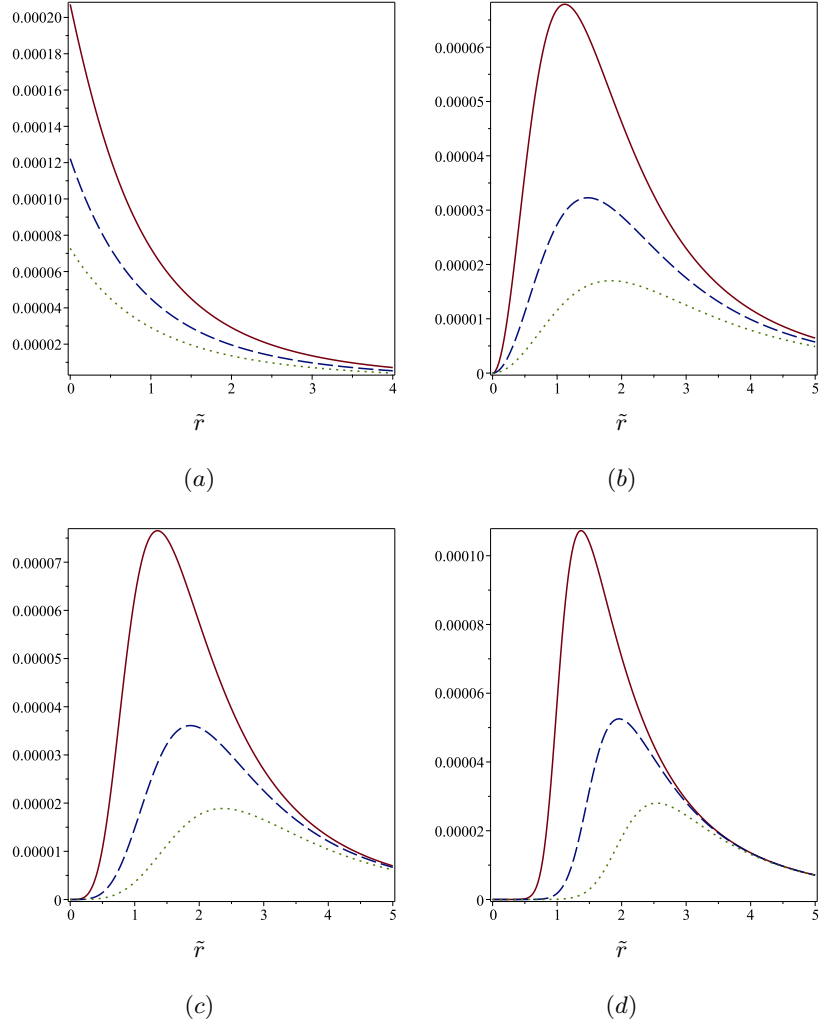


FIG. 2. The average pressure \tilde{p} , as function of \tilde{r} , for (a) the Hernquist-like model $n = 1$, (b) the Plummer-like model $n = 2$, and the shells (c) $n = 3$ and (d) $n = 6$, with parameter $\tilde{a} = 1$ (solid curves), 1.5 (dashed curves) and 2 (dotted curves).

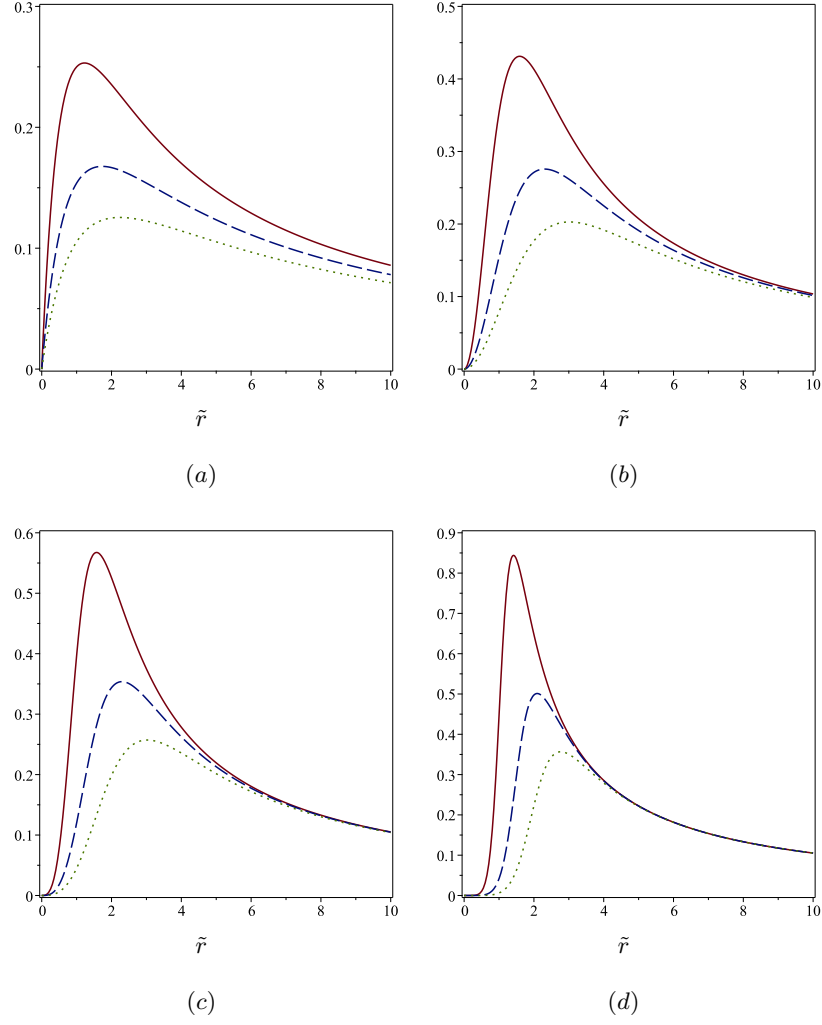


FIG. 3. The rotation curves v_c^2 , as function of \tilde{r} , for (a) the Hernquist-like model $n = 1$, (b) the Plummer-like model $n = 2$, and the shells (c) $n = 3$ and (d) $n = 6$, with parameter $\tilde{a} = 1$ (solid curves), 1.5 (dashed curves) and 2 (dotted curves).

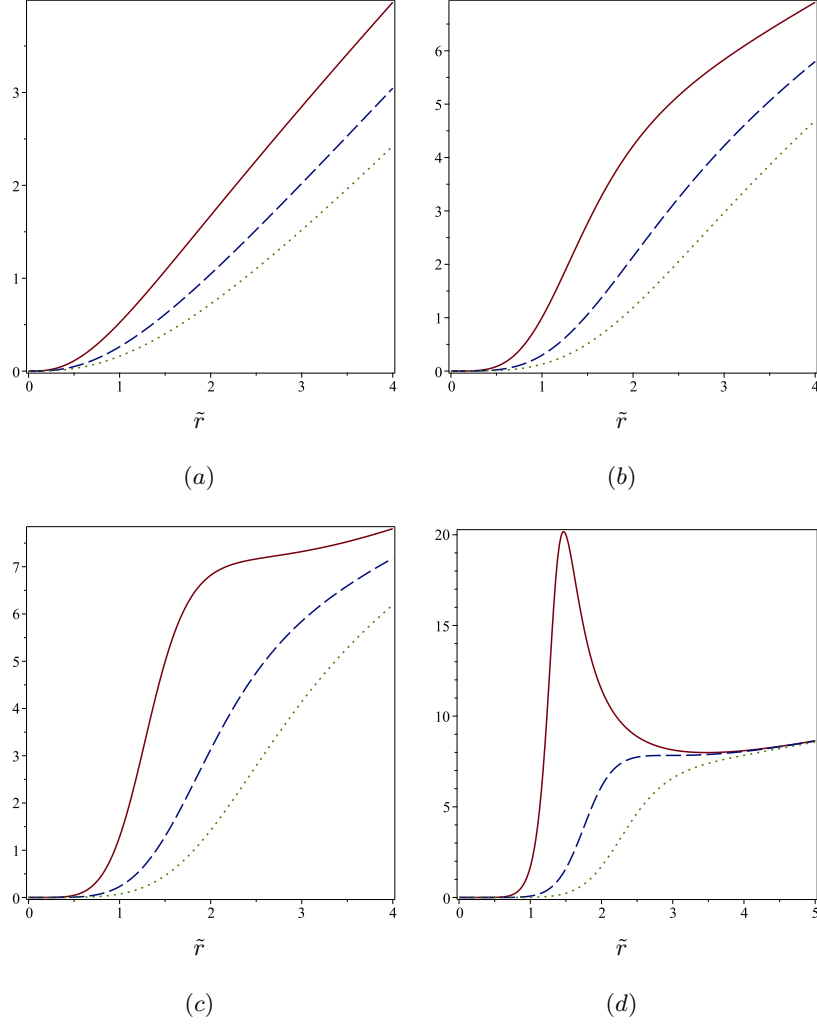


FIG. 4. The specific angular momentum \tilde{h}^2 , as function of \tilde{r} , for (a) the Hernquist-like model $n = 1$, (b) the Plummer-like model $n = 2$, and the shells (c) $n = 3$ and (d) $n = 6$, with parameter $\tilde{a} = 1$ (solid curves), 1.5 (dashed curves) and 2 (dotted curves).

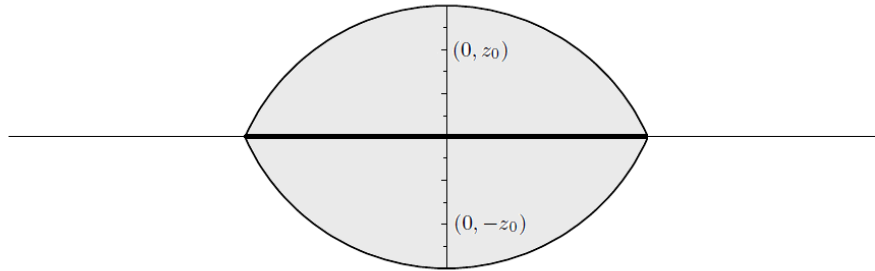


FIG. 5. Schematic representation of the system disk plus halo using the “displace, cut and reflect” method. The points $(0, -z_0)$ and $(0, z_0)$ are the centers of spheres corresponding to the spherical caps located above and below of the disk, respectively.

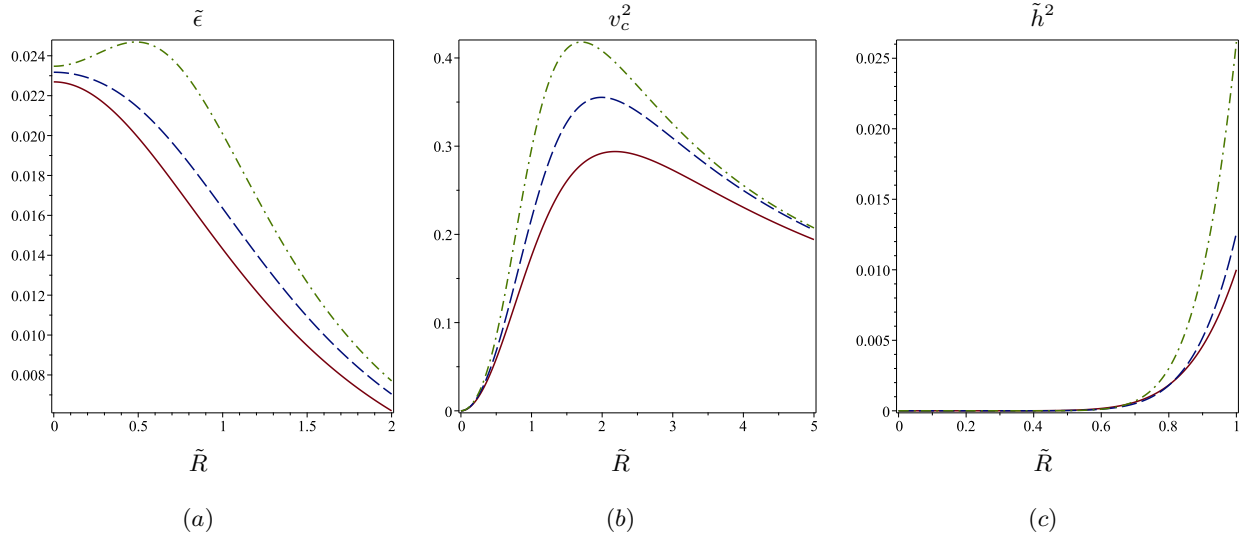


FIG. 6. (a) The surface energy density $\tilde{\epsilon}$, (b) the tangential speed (rotation curves) v_c and (c) the specific angular momentum \tilde{h} for the relativistic disk with $n = 2$ (solid curves), 3 (dashed curves), 6 (dash-dotted curves) and parameters $\tilde{a} = \tilde{z}_0 = 1$, as functions of \tilde{R}